Microporous Polymers

DOI: 10.1002/ange.200701595

Conjugated Microporous Poly(aryleneethynylene) Networks**

*Jia-Xing Jiang, Fabing Su, Abbie Trewin, Colin D. Wood, Neil L. Campbell, Hongjun Niu, Calum Dickinson, Alexey Y. Ganin, Matthew J. Rosseinsky, Yaroslav Z. Khimyak, and Andrew I. Cooper**

Dedicated to Colonel Joseph Hutchison on the occasion of his 70th birthday

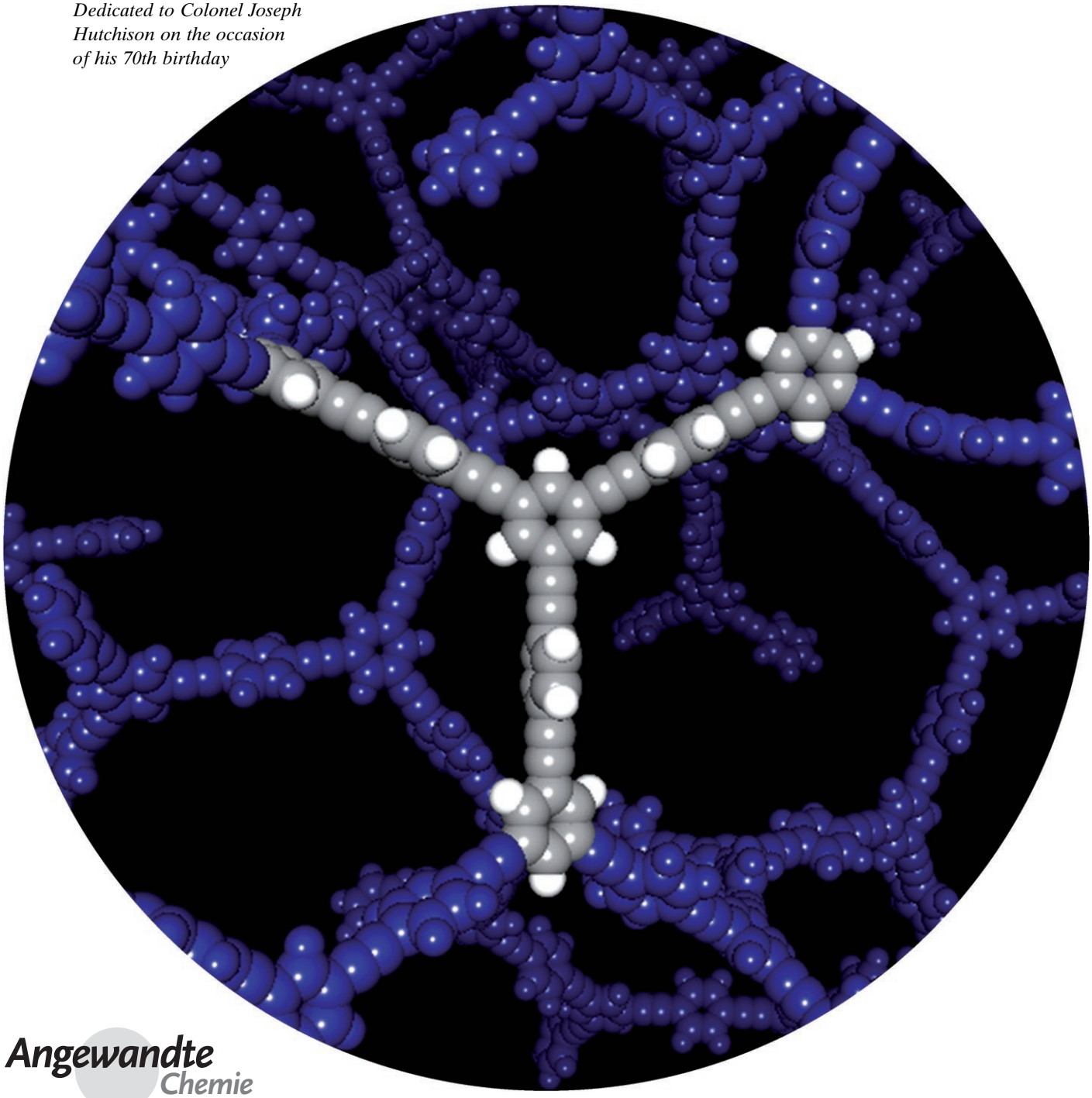

The design, synthesis, and properties of microporous framework materials have been the subject of intense recent interest, for example in the areas of gas storage and molecular separations.[1–3] In particular, there have been major advances in the preparation of crystalline metal–organic[4,5] and covalent organic[6] frameworks. We have synthesized organic conjugated poly(aryleneethynylene)[7] polymers using Sonogashira–Hagihara[8] coupling. These polymers are microporous and exhibit specific surface areas of up to 834 $m^2 g^{-1}$. Unlike metal–organic[4] and covalent organic[6] frameworks (MOFs and COFs), these conjugated microporous polymers (CMPs) are formed under kinetic control and are thus amorphous and show no long-range molecular order. Despite this lack of order, we show that it is possible to tune the micropore size distribution and surface area by varying the length of the rigid organic linkers, as demonstrated for ordered crystalline materials.[6,9] This finding suggests for the first time that order is not a prerequisite for fine control over the microporous properties of organic networks. These polyyne networks are both more thermally robust and more chemically stable than many MOFs, because they are composed solely of carbon–carbon and carbon–hydrogen bonds.

There are few methods available to synthesize substantially microporous organic polymers with large specific surface areas (greater than 700 $m^2 g^{-1}$). Hyper-cross-linked polymers are a class of amorphous microporous materials that can exhibit Brunauer–Emmett–Teller (BET) surface areas as high as 2000 $m^2 g^{-1}$.[10–12] Likewise, polymers of intrinsic microporosity (PIMs)[13,14] are rigid, contorted polymers that display permanent microporosity. Neither approach, however, has demonstrated systematic control over micropore size distribution by varying the structure of the monomers. By contrast, COFs[6] have been prepared by condensation reactions of 1,4-benzenediboronic acid (BDBA) to produce ordered crystalline microporous materials with pore sizes ranging from 0.7 to 2.7 nm. The micropore size was directly correlated to the dimensions and geometry of the precursor molecules.[6]

We have synthesized porous poly(aryleneethynylene) networks using palladium-catalyzed Sonogashira–Hagihara[8] cross-coupling, as exploited previously in the preparation of polymers,[7,15–17] molecular wires,[18,19] shape-persistent macrocycles,[20,21] and ligands for coordination-polymer synthesis.[22] The monomers employed are shown in Table 1. Each network is based on a 1,3,5-substituted benzene node connected by rigid phenyleneethynylene struts. For example, network CMP-1 consists of 1,3,5-substituted benzene nodes connected by struts containing one phenylene moiety and two ethynylene groups.[15] A series of three networks, CMP-1, CMP-2, and CMP-3, was synthesized, each possessing two ethynyl modules[23] per rigid strut, while the number of phenylene moieties in each linker increases from one (CMP-1) to three (CMP-3).

Table 1: Physical properties for polymer networks CMP-1–CMP-4.

	Alkyne monomer	Halogen monomer	S_{BET} [$m^2 g^{-1}$][a]	S_{micro} [$m^2 g^{-1}$] (t-plot)[b]	V_{micro} [$cm^3 g^{-1}$][b]	V_{tot} [$cm^3 g^{-1}$][c]	L_{av} [nm] (strut)[d]
CMP-1			834 (728)	675	0.33 (0.34)	0.47	1.107
CMP-2		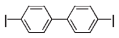	634 (562)	451	0.25 (0.24)	0.53	1.528
CMP-3	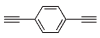	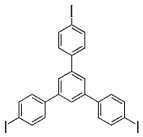	522 (409)	350	0.18 (0.17)	0.26	1.903
CMP-4	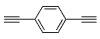		744 (645)	596	0.29 (0.26)	0.39	1.107

[a] Surface area calculated from the N_2 adsorption isotherm using the Brunauer–Emmett–Teller method (the number in parentheses is the Langmuir surface area calculated using the H_2 sorption isotherm, see text). [b] The micropore surface area and micropore volume using the t-plot method based on the Halsey thickness equation. Micropore volume in parentheses derived using the nonlocal density functional theory. [c] Total pore volume at $P/P_0 = 0.99$. [d] Average node-to-node strut length (measured between connected quaternary carbons) derived from polymer fragment models (Figure 3).

During polymerization, the networks precipitated from solution as brown powders that were totally insoluble in all solvents tested. At higher monomer concentrations, macroscopic gelation of solutions was observed, but these gels fragmented into powders upon washing and drying rather than forming stable coherent monoliths. The materials exhibited high thermal stability ($T_{dec} > 400\,°C$, see the Figures S3 and S4 in the Supporting Information) and were chemically stable, for example to acids and bases. As prepared, these networks were found to be nonconducting (pressed-pellet conductivity for CMP-1 was 10^{-12} $S cm^{-1}$). Polymers were characterized at the molecular level by ^1H–^{13}C cross-polarization magic-angle spinning (CP/MAS) NMR spectrsocopy. Assignment of the resonances (Figure 1) was confirmed using ^1H–^{13}C CP/MAS kinetics and dipolar dephasing experiments. The low-intensity lines at approximately $\delta = 76$ and 82 ppm can be ascribed to $-C{\equiv}CH$ end

[*] Dr. J.-X. Jiang, Dr. F. Su, Dr. A. Trewin, Dr. C. D. Wood, Dr. N. L. Campbell, Dr. H. Niu, Dr. C. Dickinson, Dr. A. Y. Ganin, Prof. M. J. Rosseinsky, Dr. Y. Z. Khimyak, Prof. A. I. Cooper
Department of Chemistry and Centre for Materials Discovery, University of Liverpool, Crown Street, Liverpool (UK)
Fax: (+44) 151-7942304
E-mail: aicooper@liv.ac.uk

[**] The authors gratefully acknowledge EPSRC for funding (EP/C511794/1).

Supporting information for this article is available on the WWW under http://www.angewandte.org or from the author.

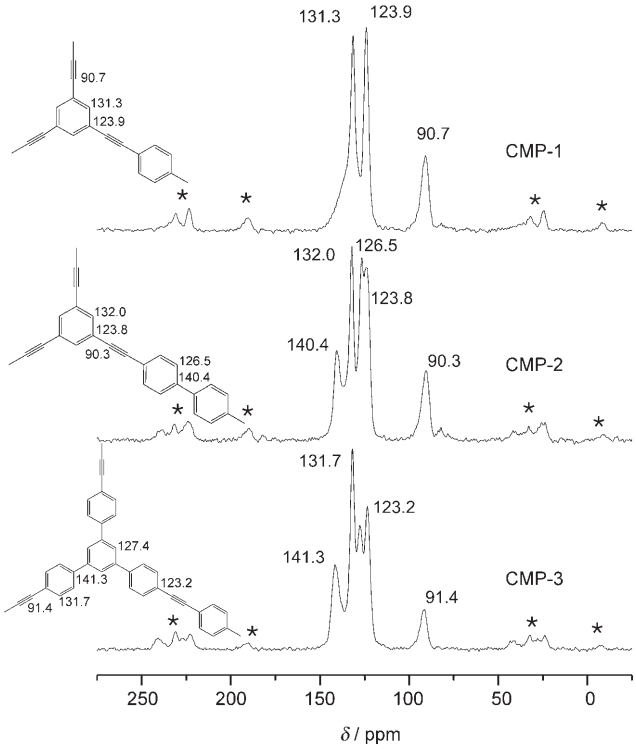

Figure 1. Solid-state NMR spectra for conjugated microporous polyyne networks. ^{1}H–^{13}C CP/MAS NMR spectra recorded at MAS rate of 10 kHz and reported relative to Me_4Si; asterisks denote spinning sidebands.

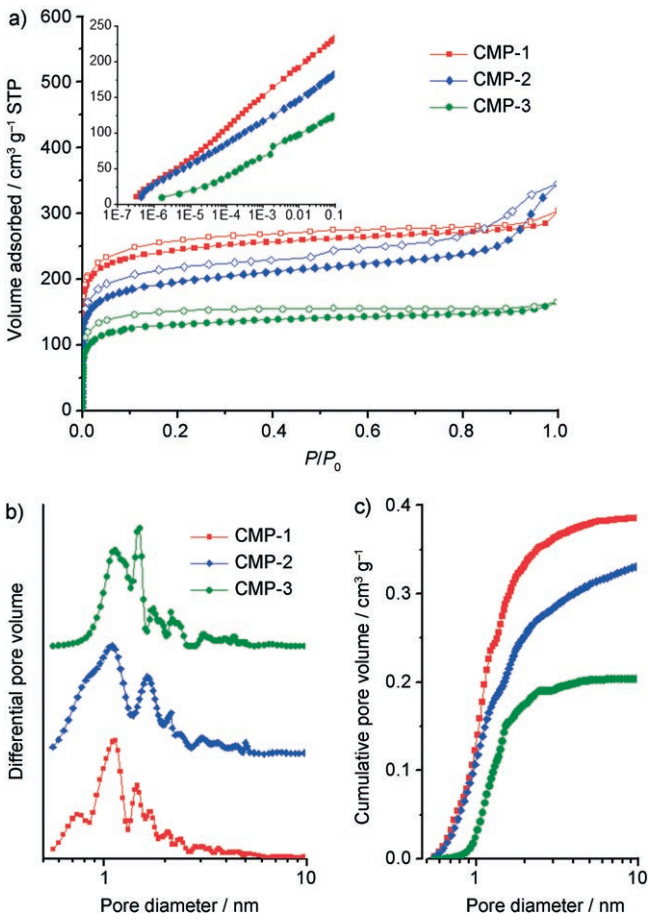

Figure 2. Nitrogen sorption analysis for microporous polyyne networks. a) N_2 adsorption–desorption isotherms measured at 77.3 K (adsorption branch is labeled with filled symbols). The inset shows a semilogarithmic plot in the pressure range $P/P_0 < 0.1$. b) Pore size distribution calculated by NLDFT. For clarity, curves have been shifted vertically. c) Cumulative pore volume calculated by NLDFT.

groups (the line at 82 ppm corresponds to a quaternary acetylene carbon atom). The ratio of intensities of aromatic to acetylene peaks was calculated using variable-contact-time ^{1}H–^{13}C CP/MAS NMR spectra with the following results: CMP-1 0.27 (expected value 0.29); CMP-2 0.18 (expected value 0.17); CMP-3 0.10 (expected value 0.15). These values were verified using $^{13}C\{^{1}H\}$ MAS NMR spectra (not shown). The spectrum of CMP-1 shows a broad shoulder at approximately 137 ppm, which may originate from the protonated carbon atoms of an aromatic end group bearing residual iodine atoms.

The porosity of the networks was investigated by sorption analyses using nitrogen (Figure 2) and hydrogen gas (see Figure S6 in the Supporting Information). All networks gave rise to type I nitrogen gas sorption isotherms according to IUPAC classifications,[24] thus indicating that the materials are microporous. The nitrogen sorption isotherm, BET surface area, and pore size distribution for CMP-1 were all similar to those observed for the covalent organic framework COF-1,[6] despite the fact that the latter material is crystalline and CMP-1 is completely amorphous (see below and Figure S7 in the Supporting Information). The BET surface area for these networks varied between 522 and 834 $m^2 g^{-1}$. The increased nitrogen uptake above a partial pressure of 0.2 and the rise in uptake at $P/P_0 > 0.8$ in the isotherm for CMP-2 may stem from interparticulate porosity associated with the complex meso- and macrostructure of this sample (Figure S9 in the Supporting Information). The inset in Figure 2a shows a semilogarithmic plot for the isotherms in the low relative pressure range ($P/P_0 < 0.01$). These data suggest that the proportion of ultramicropores (smaller than 0.7 nm) decreases in this series of samples. Figure 2b shows the nonlocal density functional theory (NLDFT) pore size distribution curves for the three networks. In general, the micropore size distribution is shifted to larger pore diameters for the series of networks CMP-1 to CMP-3. This result is shown by plots of NLDFT cumulative pore volume for the three networks (Figure 2c). These observations are consistent with the trends in physical surface areas calculated using both the BET model (N_2 as the sorbate gas) and a Langmuir model (with H_2 as the sorbate;[12] Table 1).

We have shown that the pore structure in these CMP networks can be tuned by controlling the length of the rigid connecting strut, much as for crystalline MOFs and COFs,[6,9] and that this effect was highly reproducible for repeated syntheses (see Figure S1 in the Supporting Information). To rationalize this observation, we characterized the polymers by scanning and transmittance electron microscopy (SEM and TEM) and by X-ray diffraction and carried out atomistic simulations[5,12] for network fragments. It is possible to build a number of plausible structural models for these networks,

including two-dimensional graphyne-like sheets, spiral structures, and nanotube structures, as illustrated in the Supporting Information (Figure S14). The most energetically favorable models that we found, however, were relatively disordered three-dimensional nets (Figures 3a and b).

The three-dimensional structure of the networks arises from bending of the struts out of the plane of the benzene nodes, from the dihedral angle between struts on adjacent connected nodes, from bending of the struts themselves (especially for CMP-3), and from in-plane deviation of the angle between struts from the hypothetical 120° imposed by the 1,3,5-substituted geometry. The degree of angular distortion depends on the length of the strut, L_{av} (see Table 1), the local structure of the node, and the nature of the groups within the strut. CMP-1 has the most rigid structure with the fewest interconnecting atoms ($L_{av} = 1.107$ nm; Figure 3b, left). The out-of-plane bending of struts in the CMP-1 fragment model ranges from 0° to 10°, while in-plane angles range from 115° to 130°. For the CMP-2 model, the adjacent benzene rings in the biphenyl moieties are twisted at 26°. This twist, along with an increase in L_{av} (1.528 nm), allows for greater flexibility in the structure. A wider range of in-plane and out-of-plane bending angles (108–138° and 3–26°, respectively) is observed for the struts in the CMP-2 model. The CMP-3 model contains the longest struts ($L_{av} = 1.903$ nm), and thus there is more scope for geometric distortions in the structure (Figure 3b, right). There is a broader distribution range of in-plane and out-of-plane bending angles in this model (104–138° and 3–70°, respectively). Three-dimensional nets from three-connecting ligands such as 1,3,5-benzenetricarboxylate are common in MOF chemistry and often give rise to chiral helical frameworks.[25] It should be noted that our models represent fragments of the networks rather than the pore structure itself. It is likely, for example, that there is significantly more catenation and entanglement[26,27] of fragments in the actual samples, consistent with the fact that these fragment models significantly overestimate the micropore volume.

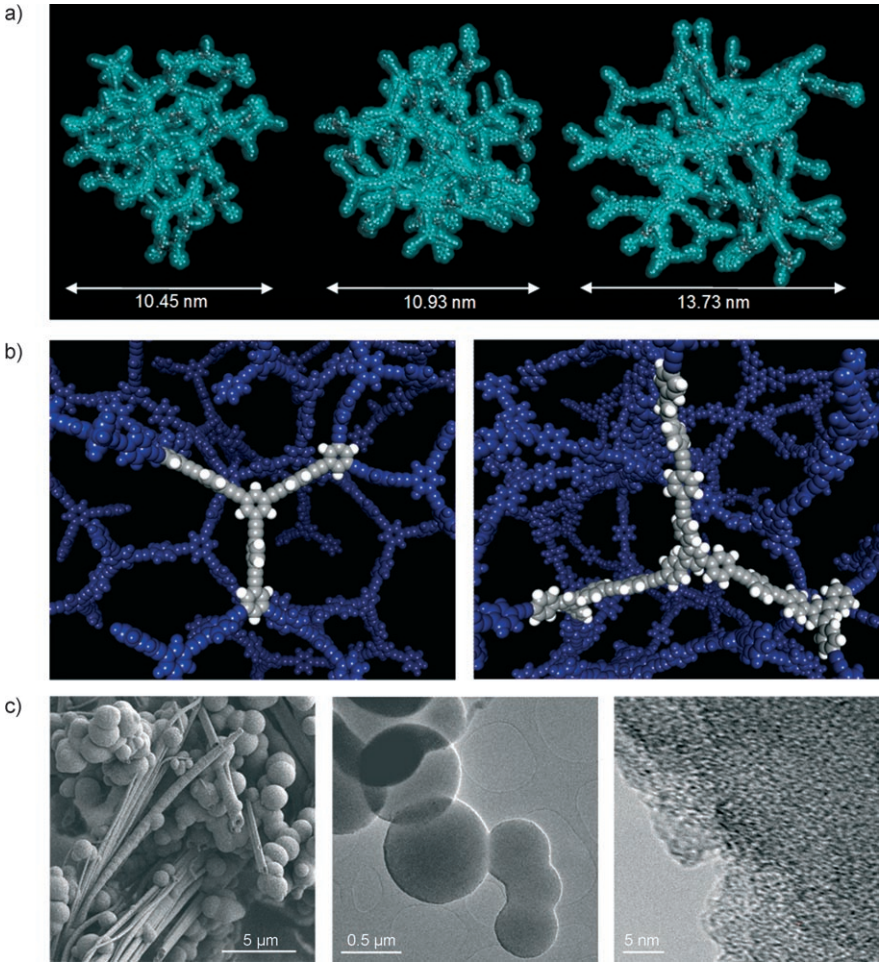

Figure 3. Atomistic simulations and microscopy for polyyne networks. a) Atomistic simulations of fragments of CMP-1 (left), CMP-2 (center), and CMP-3 (right). Each model cluster consists of 65 monomer units. A solvent-accessible surface is shown in green and was calculated using a solvent diameter of 0.182 nm. The molecular weights of these simulated fragments are 19843 (CMP-1), 29844 (CMP-2), and 34320 g mol^{-1} (CMP-3). b) Node–strut topology for simulated network fragments for CMP-1 (left) and CMP-3 (right). A 1,3,5-connected benzene node connecting three other nodes via rigid struts is highlighted in each case. c) SEM analysis for CMP-1A (left; CMP-1A: repeat synthesis of CMP-1, see the Supporting Information) and high-resolution TEM analysis for CMP-1A (middle and right).

SEM analysis revealed a complex mixed morphology for the network powders comprising both fused hollow nanotubes and solid spheres with submicrometer dimensions (Figure 3c). We do not at present have a full explanation for these specific morphologies, but nanoscale structures are not uncommon for highly cross-linked precipitation polymerization products.[12,16] X-ray diffraction (not shown) for CMP-1 revealed an amorphous halo with no evidence for characteristic reflections from a crystalline phase or layered sheets. Similarly, TEM analysis (Figure 3c) gave no evidence of ordering. There are two broad schemes for explaining microporosity in amorphous polymers; first, a homogeneous network model where the porosity is "molecular" in nature and second, a more heterogeneous model in which denser microgel particles are connected by tie chains.[12,28] Atomistic simulations, TEM analysis, gas sorption isotherms, and the correlation of micropore size with strut length all support a homogeneous, molecularly-porous network model for these materials. A fourth network, CMP-4, which was topologically equivalent to CMP-1, showed porous properties which were very similar to those of CMP-1 (Table 1, Figure S15).

In summary, we have synthesized amorphous microporous polyyne net-

works in which, like MOFs and COFs, the micropore size is closely related to the rigid monomer structure. These polymers have good chemical and thermal stability in comparison with MOF and COF materials, and there is broad scope for robust anchoring of specific functionality to the networks through carbon–carbon bond formation. The polymer networks are conjugated and there is a wealth of opportunity for producing microporous materials with useful coupled chemical, electrical, or optical properties; for example, the microporous network CMP-1 was shown to be photoluminescent[16,29] ($\lambda_{max} \approx 500$–$550$ nm, see Figure S17 in the Supporting Information). Moreover, this work challenges the notion of crystallinity being a prerequisite for molecular control over micropore size in rigid networks.

Experimental Section

Typical procedure for CMP-1: 1,3,5-triethynylbenzene (300 mg, 2.0 mmol), 1,4-diiodobenzene (659 mg, 2.0 mmol), tetrakis-(triphenylphosphine)palladium (100 mg), and copper iodide (30 mg) were dissolved in a mixture of toluene (3 mL) and Et_3N (3 mL). The reaction mixture was heated to 80 °C, stirred for 24 h under a nitrogen atmosphere, and then cooled to room temperature (see the Supporting Information for details).

Details of gas sorption, SEM, TEM, and NMR spectroscopy experiments are given in the Supporting Information. For atomistic simulations, molecular models for the network fragments were generated using the Materials Studio Modeling 4.0 package (Accelrys Inc., San Diego, CA, 2005; see the Supporting Information). All models fully relaxed using the *Discover* molecular mechanics and dynamics simulation module with the COMPASS forcefield.[30]

Received: April 11, 2007
Revised: July 15, 2007
Published online: September 26, 2007

Keywords: conjugation · microporous materials · networks · polymerization

[1] S. Kitagawa, R. Kitaura, S. Noro, *Angew. Chem.* **2004**, *116*, 2388; *Angew. Chem. Int. Ed.* **2004**, *43*, 2334.
[2] O. M. Yaghi, H. L. Li, C. Davis, D. Richardson, T. L. Groy, *Acc. Chem. Res.* **1998**, *31*, 474.
[3] A. K. Cheetham, G. Férey, T. Loiseau, *Angew. Chem.* **1999**, *111*, 3466; *Angew. Chem. Int. Ed.* **1999**, *38*, 3268.
[4] H. Li, M. Eddaoudi, M. O'Keeffe, O. M. Yaghi, *Nature* **1999**, *402*, 276.
[5] C. Mellot-Draznieks, G. Férey, *Prog. Solid State Chem.* **2005**, *33*, 187.
[6] A. P. Côté, A. I. Benin, N. W. Ockwig, M. O'Keeffe, A. J. Matzger, O. M. Yaghi, *Science* **2005**, *310*, 1166.
[7] U. H. F. Bunz, *Chem. Rev.* **2000**, *100*, 1605.
[8] K. Sonogashira, Y. Tohda, N. Hagihara, *Tetrahedron Lett.* **1975**, *16*, 4467.
[9] M. Eddaoudi, J. Kim, N. Rosi, D. Vodak, J. Wachter, M. O'Keefe, O. M. Yaghi, *Science* **2002**, *295*, 469.
[10] M. P. Tsyurupa, V. A. Davankov, *React. Funct. Polym.* **2006**, *66*, 768.
[11] J. Y. Lee, C. D. Wood, D. Bradshaw, M. J. Rosseinsky, A. I. Cooper, *Chem. Commun.* **2006**, 2670.
[12] C. D. Wood, B. Tan, A. Trewin, H. Niu, D. Bradshaw, M. J. Rosseinsky, Y. Z. Khimyak, N. L. Campbell, R. Kirk, E. Stoeckel, A. I. Cooper, *Chem. Mater.* **2007**, *19*, 2034.
[13] P. M. Budd, B. S. Ghanem, S. Makhseed, N. B. McKeown, K. J. Msayib, C. E. Tattershall, *Chem. Commun.* **2004**, 230.
[14] N. B. McKeown, B. Gahnem, K. J. Msayib, P. M. Budd, C. E. Tattershall, K. Mahmood, S. Tan, D. Book, H. W. Langmi, A. Walton, *Angew. Chem.* **2006**, *118*, 1836; *Angew. Chem. Int. Ed.* **2006**, *45*, 1804.
[15] D. L. Trumbo, C. S. Marvel, *J. Polym. Sci. Part A* **1986**, *24*, 2311.
[16] E. Hittinger, A. Kokil, C. Weder, *Angew. Chem.* **2004**, *116*, 1844; *Angew. Chem. Int. Ed.* **2004**, *43*, 1808–1811.
[17] J. D. Mendez, M. Schroeter, C. Weder, *Macromol. Chem. Phys.* **2007**, *208*, 1625.
[18] Z. J. Donhauser, B. A. Mantooth, K. F. Kelly, L. A. Bumm, J. D. Monnell, J. J. Stapleton, D. W. Price, A. M. Rawlett, D. L. Allara, J. M. Tour, P. S. Weiss, *Science* **2001**, *292*, 2303.
[19] Q. Zhou, T. M. Swager, *J. Am. Chem. Soc.* **1995**, *117*, 12593.
[20] D. Venkataraman, S. Lee, J. S. Zhang, J. S. Moore, *Nature* **1994**, *371*, 591.
[21] W. Zhang, J. S. Moore, *Angew. Chem.* **2006**, *118*, 4524; *Angew. Chem. Int. Ed.* **2006**, *45*, 4416.
[22] Y. H. Kiang, G. B. Gardner, S. Lee, Z. T. Xu, E. B. Lobkovsky, *J. Am. Chem. Soc.* **1999**, *121*, 8204.
[23] P. F. H. Schwab, M. D. Levin, J. Michl, *Chem. Rev.* **1999**, *99*, 1863.
[24] K. S. W. Sing, D. H. Everett, R. A. W. Haul, L. Moscou, R. A. Pierotti, J. Rouquerol, T. Siemieniewska, *Pure Appl. Chem.* **1985**, *57*, 603.
[25] D. Bradshaw, T. J. Prior, E. J. Cussen, J. B. Claridge, M. J. Rosseinsky, *J. Am. Chem. Soc.* **2004**, *126*, 6106.
[26] T. M. Reineke, M. Eddaoudi, D. Moler, M. O'Keeffe, O. M. Yaghi, *J. Am. Chem. Soc.* **2000**, *122*, 4843.
[27] O. M. Yaghi, *Nat. Mater.* **2007**, *6*, 92.
[28] C. Urban, E. F. McCord, O. W. Webster, L. Abrams, H. W. Long, H. Gaede, P. Tang, A. Pines, *Chem. Mater.* **1995**, *7*, 1325.
[29] T. Yamamoto, W. Yamada, M. Takagi, K. Kizu, T. Maruyama, N. Ooba, S. Tomaru, T. Kurihara, T. Kaino, K. Kubota, *Macromolecules* **1994**, *27*, 6620.
[30] H. Sun, *J. Phys. Chem. B* **1998**, *102*, 7338.

